RSC Advances

PAPER

View Article Online
View Journal | View Issue

Cite this: *RSC Adv.*, 2023, **13**, 21063

Preparation of Ru/N-doped carbon catalysts by induction of different nitrogen source precursors for the hydroprocessing of lignin oil†

Yudan Zhong, Yulong Ma,* Yonggang Sun,* Liqiong Wang, Yuanyuan Li, Feng Lin and Yingbo Zhu

The lignin oil produced by rapid pyrolysis of lignin is considered a promising liquid fuel source. Hydrodeoxygenation (HDO) is a kind of efficient method to upgrade the lignin oil, and a high-performance catalyst is key to the hydrodeoxygenation of lignin oil. In this study, a high dispersion and small size Ru nanoparticle loaded N-doped carbon catalyst was derived by the direct pyrolysis of a mixture of ruthenium trichloride and melamine, and it could efficiently convert lignin oil. The lignin oil was completely transformed at 240 °C and 1 MPa H_2, and 36.58% cyclohexane was obtained. The formation, surface area, and nitrogen species of the catalyst could be controlled by changing the precursor of the nitrogen-doped carbon support. The percentage of pyridine nitrogen possessed with melamine as a nitrogen–carbon precursor (31.35%) was much higher than that with urea (16.47%) and dicyandiamide (8.20%) as nitrogen–carbon precursors. The presence of pyridine nitrogen could not only serve as the coordination site for even dispersity and stability of Ru nanoparticles but also regulated the electron density of Ru nanoparticles (NPs) and increased the active site Ru^0 through electron transfer.

Received 22nd March 2023
Accepted 28th June 2023

DOI: 10.1039/d3ra01866k

rsc.li/rsc-advances

Introduction

As the world population increases, leading to the rapid consumption of fossil fuels, there is an urgent need to develop safe, clean, efficient, and renewable sources.[1] Lignin is the second most abundant biopolymer in biomass, and it is a renewable resource of aromatic compounds in nature,[2] and is considered a renewable alternative to traditional fossil fuels.[3] In addition, pulping and paper industries also contribute approximately 50 million tons of lignin "waste" annually.[4] As the most abundant natural aromatic, lignin can serve as a potentially valuable source for the production of biofuels, energy, and chemicals. Thus, the effective depolymerization of lignin into aromatics would greatly improve the economics of the overall biorefinery process.[5] However, the utilization of lignin is low and there is a need to develop efficient ways and methods to utilize lignin.

Lignin is a phenylpropane structure linked by C–C and C–O bonds, where C–O bonds account for two-thirds of the total number of bonds, and the dissociation energy is lower than that of C–C bonds. Hence, breaking aromatic C–O bonds is crucial for valorizing lignin to fuels/value-added chemicals.[6] The depolymerization methods of lignin mainly include pyrolysis,[7] hydrolysis,[8] hydrogenolysis,[9] and oxidation.[10] Metal-based catalysts are the common choices to complete the hydrogenolysis process due to the high catalytic activity of the metal sites,[11] Such as Ru-,[12] Ni-,[13] Pd-,[14] Pt[15]-based catalysts. Activated carbon is the most widely used catalyst carrier because of its easy availability and low cost. However, the absence of adequate anchoring sites in activated carbon leads to the aggregation and reduction of metal NPs. Therefore, highly active carriers have aroused great interest in the preparation of supported metal catalysts for lignin conversion.

The lignin oil produced using either pyrolysis has been considered a clean and environmentally friendly energy fuel as its combustion generates lower greenhouse gas emissions compared to the conventional fossil fuels.[16] However, due to the high content of water and oxygen, low heating value and low stability of pyrolytic lignin oil, it is very difficult to directly utilize pyrolytic lignin oil.[17] Therefore, it is very important to upgrade pyrolytic lignin oil. The most efficient way to upgrade pyrolysis lignocellulosic oil is hydrodeoxygenation,[18] which

State Key Laboratory of High-efficiency Coal Utilization and Green Chemical Engineering, College of Chemistry and Chemical Engineering, Ningxia University, Yinchuan, China. E-mail: yulongma796@sohu.com; cassyg2015@163.com

† Electronic supplementary information (ESI) available: TEM images of Ru/NC-M (Fig. S1); N_2 adsorption isotherm (Fig. S2); XPS spectra of catalysts N 1s (Fig. S3); hydrogenolysis of lignin oil over different catalysts (Fig. S4); ICP-MS analysis for the Ru/N-doped carbon catalysts (Table S1); BET surface area, pore volume and pore diameter of catalysts (Table S2); the various Ru species content of the Ru/N-doped carbon catalysts (Table S3); the data of pyridine-IR (Table S4); the comparison of catalytic performance between the Ru/NC-M and previous reported catalysts (Table S5); graphical abstract (Fig. S5). See DOI: https://doi.org/10.1039/d3ra01866k

can remove oxygen and H_2 in lignocellulosic oil in the form of H_2O, while in the cracking process, oxygen in lignocellulosic oil is mainly removed in the form of CO_2 and CO, thus reducing the total carbon production.[19]

In recent years, the nitrogen-doped carbon carrier metal catalysts have attracted extensive interest because nitrogen doping can improve the catalytic activity by enhancing the electronic interaction between the metal and carbon carriers and changing the acid–base properties of the carrier surface.[20] Yang *et al.*[21] synthesized a series of N-doped carbon (NC-x) carriers with high nitrogen content, prepared Ru/NC-x catalysts by ultrasound-assisted impregnation, and converted nitrobenzene to aniline at room temperature, and nitrogen doping highly dispersed ruthenium nanoparticles, forming electron-deficient ruthenium species. Li *et al.*[22] synthesized a Ru@N-doped carbon catalyst by two-stage pyrolysis of carbon-nitrogen precursor and ruthenium trichloride mixture, which showed favorable catalytic activity for the cracking of C–O bonds in lignin with a total aromatic monomer yield of 30.5%, and the incorporation of pyridine or pyrrole N atoms on graphitic carbon support can not only uniformly disperse and stabilize Ru nanoparticles (NPs) but also produce defect-free carbon structures. Jacky *et al.*[23] presented a facile methodology for the *in situ* formation of palladium nanoparticles by reduced gases produced by the pyrolysis of bio-polymeric marine waste, chitosan resulting in the N-doped carbon support. The incorporation of nitrogen into the carbon framework served as a nucleation site for the uniform and stabilized palladium metal dispersion.

While the reported noble metal-based catalysts (such as Pd/C,[14] and Au/CdS[24]) had excellent catalytic properties, they were more expensive and had limitations in large-scale applications. Non-precious metal catalysts were low cost, but when used for hydrogenolysis of lignin oils, a high metal loading was required for high conversion and selectivity. Compared with monometallic catalysts, bimetallic catalyst[25] showed stronger catalytic performance, with significantly improved conversion and monomer selectivity. However, the preparation process of bimetallic catalyst was more complex, and the catalyst stability needs to be increased further. In this work, it was concluded that the Ru/N-doped carbon catalyst could exhibit excellent catalytic performance for lignin oil under milder reaction conditions and the metal Ru was less expensive than other noble metals (such as Pd and Pt). Therefore, Ru was a suitable hydrogenolysis metal for the conversion of lignin oil.

In this paper, the Ru/NC-M catalyst with strong metal support interaction was prepared by *in situ* direct pyrolysis of a mixture of melamine and $RuCl_3 \cdot xH_2O$. This Ru/NC-M catalyst could achieve efficient conversion of lignin oil under relatively mild conditions. The pyridine in the carrier remodels the electron density of Ru NPs and offers more Ru^0 active sites through electron interactions. Therefore, the catalyst exhibited superior catalytic activity in the hydrogenolysis of lignin oil.

Experimental

Materials

The reagents used in this experiment are all analytical grade. Ruthenium chloride hydrate ($RuCl_3 \cdot xH_2O$, 30%), melamine, dicyandiamide, guaiacol and Ru/C (Ru was 5 wt%) were purchased from Aladdin reagent. Urea ($CO(NH_2)_2$), ethyl acetate and isopropanol were purchased from Sinopharm Chemical Reagent Co., Ltd. Straw lignin is purchased from Shandong Longli Co., Ltd.

Preparation of catalysts

Ru/NC catalyst is prepared by the one-pot method. The weighed 50 mg $RuCl_3 \cdot xH_2O$ and 5 g of urea, dicyandiamide, and melamine were put into a mortar for grinding, and the ground powder was put into a crucible, and calcined for 2 h at 500 °C, 600 °C and 650 °C in a muffle furnace. The calcined sample powder was placed in an H_2 tube furnace, calcined at 300 °C for 2 h (heating rate was 5 °C min^{-1}), and passed by 1% O_2/N_2 for 2 h after the temperature was reduced to room temperature. The prepared catalysts were named Ru/NC-U, Ru/NC-D, and Ru/NC-M. Urea, dicyandiamide, and melamine were put into the muffle furnace for calcination respectively to obtain a carrier without added metal, which was named NC-U, NC-D, and NC-M.

Preparation of lignin oil

The straw lignin used in this study was purchased from Shandong Longli Co., Ltd. The straw lignin was dried and ground before the experiment. The pyrolysis of straw lignin was carried out at a rapid heating rate of 30 °C min^{-1} in a nitrogen atmosphere to 550 °C. After pyrolysis, the liquid collected was extracted with 30 mL ethyl acetate to remove the water phase, and then the ethyl acetate was removed with a rotary evaporator to obtain dark brown liquid lignin oil. GC-FID (Shimadzu GC-2014, CAP-5, 30 m × 250 μm × 0.25 μm) and GC-MS (Agilent, 7890B/5977C, 60 m × 250 μm × 0.25 μm) were used for qualitative and quantitative analysis of lignin oil. The initial furnace temperature was 45 °C and kept for 1 min. Then the temperature was raised to 120 °C at 20 °C min^{-1} and then to 280 °C at 50 °C min^{-1} for 2 min.

Degradation of lignin oil

100 mg of lignin oil, 50 mg of catalyst, and 30 mL of isopropanol were added to a 100 mL stainless steel autoclave (Beijing Century Senlang Chemical Co., Ltd., China). After the reactor is purged three times with nitrogen, it is filled with 1 MPa hydrogen. Then, the catalytic reaction is performed at 240 °C and 800 rpm. Immediately after the reaction, the reactor is cooled to room temperature with an ice bath, and the liquid products are collected for further study. All experiments were repeated three times. The reaction products were qualitatively analyzed by gas chromatography (Shimadzu GC-2014, CAP-5, 30 m × 250 μm × 0.25 μm) using a hydrogen flame ionization detector (FID). The injector and detector temperature was 280 °

C and the injection volume was 2 μL. The external standard method was used to calculate the conversion rate of the reactants, the selectivity of the product, and the yield. The calculation was as follows:

$$\text{Conversion} = (n_{\text{initial}} - n_{\text{remaining amount after reaction}})/n_{\text{initial}} \times 100\% \quad (1)$$

$$\text{Product selectivity} = n_{\text{product}}/n_{\text{total product}} \times 100\% \quad (2)$$

where n is the molar mass.

Catalyst characterization

On an X-ray diffractometer (dmax2200pc, Rigaku), X-ray diffraction (XRD) spectra of the sample were obtained using Cu kα1 radiation ($\lambda = 1.540$ Å) at 40 kV and 40 mA. And scan in the range of 3–85°. The metal content was measured on ICP-MS (Aglient 7800). The sample and the acid solvent were mixed and then microwave digestion was performed to measure the metal content in the sample. The morphology of the catalyst was characterized by SEM (Czech Republic TESCAN MIRA LMS). The morphology and metal particle size of the catalyst was characterized by transmission electron microscopy (TEM, FEI Talos F200x, USA). The nitrogen adsorption and desorption curve, specific surface area, and pore structure characteristics of the sample were obtained by using the automatic specific surface area and porosity analyzer (ASAP2460, Micromeritics, USA). Using the Thermo ESCALAB 250XI device, X-ray photoelectron spectroscopy (XPS) of the sample was obtained. The type of acidity (Lewis acid and Brønsted acid) on the catalyst surface was measured using pyridine infrared (Tensor 27). The structural characteristics of lignin oil samples and depolymerized products were studied using a 2D HSQC method (Bruker-Avance III 600 MHz spectrometer, Germany), and the lignin oil samples were tested after dissolution with deuterated dimethyl sulfoxide (DMSO) with a scan number of 32 and a relaxation time of 1.5 s. Using the Netzsch TG 209 F3 Tarsus device, TG of the sample was obtained.

Results and discussion

Characterization of catalysts

Ru/NC catalysts (Ru/NC-U, Ru/NC-D, and Ru/NC-M) were prepared by pyrolysis of ruthenium trichloride and urea, dicyandiamide, and melamine mixtures, respectively. The actual content of Ru determined according to ICP-MS was 6.40 wt%, 7.50 wt%, and 3.24 wt%, respectively (Table S1†). Through SEM characterization, it could be seen that the topography of Ru/NC-U has no obvious layered structure (Fig. 1a), and the topography of Ru/NC-D and Ru/NC-M was a folded layered structure (Fig. 1b and c), meanwhile, the partial metal agglomeration could be only observed in Ru/NC-D. In the process of pyrolysis, firstly, the melamine was coagulated into layered graphitic carbon nitride (g-C_3N_4) and a carbon skeleton at 600 °C, respectively. The morphology of the wrinkled nanosheets originated from the morphology of the g-C_3N_4.[26] For further carbonization at the higher temperature volatile gases

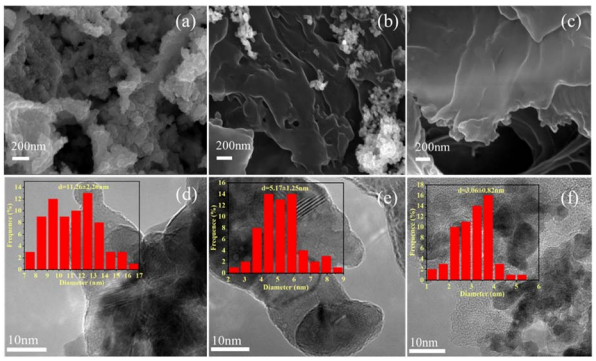

Fig. 1 SEM images of (a) Ru/NC-U, (b) Ru/NC-D, (c) Ru/NC-M, TEM images of (d) Ru/NC-U, (e) Ru/NC-D, (f) Ru/NC-M.

from the decomposition of g-C_3N_4 was generated.[27] According to the transmission electron microscopy (TEM) results, it could be seen that there was an agglomeration of metal Ru on Ru/NC-D and Ru/NC-U catalysts (Fig. 1e and d), and the average size of Ru NPs was 11.26 and 7.09 nm, respectively. For Ru/NC-M catalyst, the metal Ru was uniformly distributed on the support (Fig. 1f), and the average size of Ru NPs is 3.06 nm, which was much smaller than the average size of Ru/NC-U and Ru/NC-D, the proportion of pyridine nitrogen bound to Ru/NC-M was the highest, 31.35%, which was much higher than that of Ru/NC-U (16.47%) and Ru/NC-D (8.20%), so the presence of pyridine nitrogen can make the metal have better dispersion.

X-ray diffraction (XRD) spectroscopy was used to elucidate the crystal structures of various catalysts (Fig. 2), the diffraction peaks of Ru/NC-U and Ru/NC-D at 2θ of 38.39°, 42.15°, and 44.00° were ascribed to the (100), (002) and (101) crystal planes of Ru, respectively (PDF#06-0663). It was also shown that Ru exists as a (002) crystal plane (Fig. S1†). However, these feature peaks of Ru/NC-M were extremely small, indicating that Ru NPs were well dispersed on the NC-M carrier, while Ru might be agglomerated on the NC-U and NC-D carriers.[12] According to the measured N_2 adsorption–desorption isotherms (Fig. S2†), all catalysts showed similar type III N_2 adsorption–desorption isotherms, of which only Ru/NC-M showed a significant hysteresis loop, demonstrating the presence of a mesoporous structure.[28] Ru/NC-U and Ru/NC-D did not show a significant

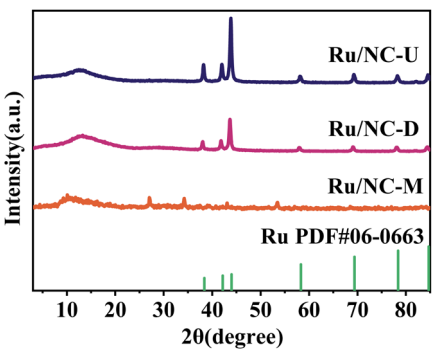

Fig. 2 XRD of catalysts.

hysteresis loop probably because of the relatively small specific surface area. The specific surface areas of Ru/NC-U, Ru/NC-D, and Ru/NC-M had specific surface areas of 2.2, 2.6, and 8.6 $m^2\ g^{-1}$, respectively (Table S2†).

The surface chemical composition and chemical states of the surface elements in Ru/NC-U, Ru/NC-D, and Ru/NC-M were investigated based on XPS analysis. Four peaks with binding energies of 399.34 eV, 399.96 eV, 400.97 eV, and 402.10 eV could be distinguished from different N species according to the high-resolution N 1s spectra (Fig. S3†), which were pyridine N, pyrrole N, graphite N, and N-oxide.[22,29] The total nitrogen content in Ru/NC-U, Ru/NC-D, and Ru/NC-M decreased sequentially (Fig. 3a), and pyridine N in Ru/NC-U and Ru/NC-D, accounting for 16.47% and 8.20% of the total nitrogen species, respectively.

However, pyridine N dominated in Ru/NC-M, accounting for 31.35% of the total nitrogen species (Table 1). The peak of 398.25 eV might contain the role of nitrogen in the metal–N bond, which was due to the fact that the binding energies of pyridine N and Ru-Nx were very close to each other, making it difficult to distinguish quantitatively.[30] The proportion of distinct nitrogen species varied with NC precursors. The high-resolution Ru 3p spectrum (Fig. 3b) showed four peaks with binding energies of 462.00 eV and 484.24 eV assigned to Ru^0 $3p_{3/2}$ and Ru^0 $3p_{1/2}$, and binding energies of 464.23 eV and 486.13 eV assigned to Ru^{n+} $3p_{3/2}$ and Ru^{n+} $3p_{1/2}$.[31] Among the three catalysts, Ru/NC-M had the highest Ru^0 content of 71.94%, while Ru/NC-U and Ru/NC-D had 65.50% and 59.14% of Ru^0, respectively (Table S3†). As the percentage of pyridine nitrogen increased, the content of Ru^0 also increased, indicating that the dominant pyridine nitrogen could regulate the electron density of Ru NPs and increase the active site Ru^0 through electron transfer,[29] Therefore the Ru/NC-M catalysts possessed stronger catalytic performance.

In addition, the Brønsted acid and Lewis acid distributions were measured by pyridine adsorption IR (Py-IR). The acidity distribution of the catalyst was analyzed based on pyridine infrared and the concentrations of Brønsted (B) and Lewis (L) acid centers in the catalyst were quantitated (Fig. 4a). The bands at around 1450 cm^{-1} and 1596 cm^{-1} were ascribed to the adsorption of pyridine on the Lewis acidic site, the bands at around 1544 cm^{-1} and 1650 cm^{-1} were ascribed to the adsorption of pyridine on the Brønsted acidic site, and the band at around 1490 cm^{-1} was ascribed to the adsorption of pyridine on both the Lewis acidic site and the Brønsted acidic site.[13,32]

Table 1 The various N species content of the Ru/N-doped carbon catalysts

Catalyst	Pyridinic N	Pyrrolic N	Graphitic N	N-oxide
Ru/NC-U	16.47	10.23	29.47	43.83
Ru/NC-D	8.20	10.60	27.90	53.30
Ru/NC-M	31.35	22.03	21.66	24.95

The distribution of lignin oil hydrolysis products depended on the acidity of the catalyst. It could be clearly seen that Ru/NC-M catalyst owned a higher amount of Lewis acid, Brønsted acid, and total acid than Ru/NC-U and Ru/NC-D catalysts (Table S4†), and the selectivity for cyclohexane was also the highest. A synergistic interaction between Lewis and Brønsted acid sites and hydrogen donors was reported to show intensive hydrogen production.[32] Reactive hydrogen species would further attack the C–O bond. In addition, the Brønsted acidic site promoted the removal of the –OH group,[33] and the Lewis acidic site promoted the removal of the O–CH_3 group.[34] Therefore, a suitable increase in acidity could lead to a good catalytic performance. Furthermore, the increase of total and Brønsted acids of the catalyst was shown to be necessary for the cleavage of C–O bonds in lignin, which can favor the hydrogenolysis of lignin-derived dimers.[35] Thermal gravity analysis is an effective way to determine the thermal stability of the samples. The weight loss below 100 °C was due to the removal of surface water molecules. A steep curve from 323 to 421 °C is observed, and the weight loss at this stage is rapid, which can be ascribed to the sublimation of melamine (Fig. 4b).

Hydrogenolysis of lignin oil

To investigate the role of carriers in the hydrogenolysis of lignin oil (Table 2), carriers without loaded metal Ru (NC-U, NC-D, and NC-M) were added to the hydrogenolysis reaction, and the conversion of lignin oil was found to be extremely low, all less than 3%, which indicated that the carriers were not active for the hydrogenolysis of lignin oil, thus it showed that the synergistic effect between metal Ru^0 and nitrogen-doped carbon carriers played a key role in the degradation of lignin oil.

The results showed that the synergistic effect between Ru^0 and nitrogen-doped carbon support plays a key role in the degradation of lignin oil. In addition, hydrodeoxygenation of

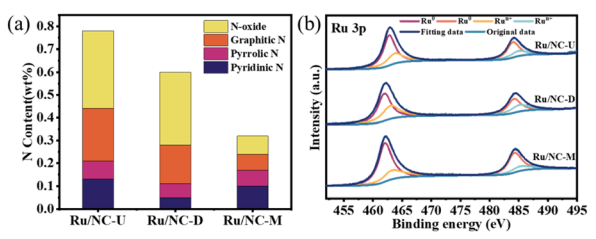

Fig. 3 XPS spectra of catalysts (a) proportion of each nitrogen species and (b) Ru 3p.

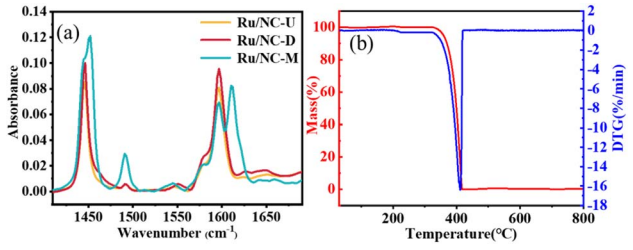

Fig. 4 (a) Pyridine-IR acidity distribution of the samples, (b) TG of Ru/NC-M.

Table 2 Hydrodeoxygenation reaction of lignin oil over different catalysts[a]

Catalyst	Conversion (%)	Product selectivity (%)				
		1	2	3	4	5
Blank	0	0	0	0	0	0
NC-U	1.88	0	0	0	0	100
NC-D	1.37	0	0	0	0	100
NC-M	2.57	0	0	35.01	0	64.99
Ru/C	7.00	92.42	0	7.58	0	0
Ru/NC-U	100	13.79	7.86	36.17	12.42	29.77
Ru/NC-D	100	7.70	6.49	40.48	15.26	30.08
Ru/NC-M	100	36.58	5.01	27.85	12.17	18.39

[a] Reaction conditions: 50 mg lignin oil, 25 mg catalyst, 30 mL isopropanol, 240 °C, 1 MPa H_2, 7 h, 800 rpm.

lignin oil with Ru/C catalyst (Ru was 5 wt%) revealed that the conversion of lignin oil was less than 10%. Therefore, the presence of nitrogen could enhance the activity of the catalyst.

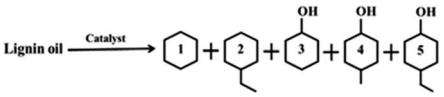

After the straw lignin was pyrolyzed into lignin oil, the monomer products were extracted with ethyl acetate and then subjected to GC and GC-MS analysis. The main phenolic monomer products produced were phenol (A), guaiacol (B), 4-ethylphenol (C), 4-ethyl guaiacol (D), 2,6-dimethoxyphenol (E), and 4-ethylcatechol (F) (Fig. 5a). Lignin oil was hydrogenated in isopropanol at 240 °C, 1 MPa H_2, and different catalysts for 7 h, and the product compositions were shown in Table 2, Ru/NC-U and Ru/NC-D showed the highest selectivity for cyclohexanol with 36.17% and 40.48%, respectively, while Ru/NC-M showed the highest selectivity for cyclohexane with 36.58%. The results indicated that Ru/NC-M had a stronger ability to break the C–O bond. Compared with the selectivity of cyclohexane it was found that Ru/NC-M had the highest selectivity for cyclohexane and the strongest ability to remove hydroxyl groups, probably the most B acidic sites, which would accelerate the dehydration of cyclohexanol to obtain cyclohexane.[36] Compared with Ru/NC-U and Ru/NC-D, Ru/NC-M had a greater specific surface area and enriched mesopores, which could be attributed to the presence of mesoporous structures that could facilitate mass transfer and diffusion of lignin oil in the catalyst.[37] On the other hand, the Ru/NC-M catalyst with the highest percentage of pyridine nitrogen in the total nitrogen species provided more Ru^0 active sites and therefore stronger catalytic activity. The effect of reaction time on the degradation of lignin oil over Ru/NC-M catalyst was investigated (Fig. 5b). The products at the beginning of the reaction were only cyclohexane, cyclohexanol and 4-ethylcyclohexanol with selectivity of 9.91%, 65.68%, and 24.41%, respectively, and conversion of 41%. As the reaction time continued, in addition to cyclohexane, cyclohexanol, and 4-ethylcyclohexanol, ethyl cyclohexane and 4-methyl cyclohexanol were also generated, and the conversion of lignin oil gradually elevated, the content of cyclohexane gradually increased, and the content of cyclohexanol gradually decreased, which showed that Ru/NC-M could effectively break the C–O bond, and finally the lignin oil was completely converted at 7 h of the reaction.

Since the reusability of catalysts was critical for commercial applications, recovery and reusability of catalysts were investigated under the same reaction conditions (Fig. 5c). At the end of each reaction cycle, the solid catalyst was filtered, washed with deionized water aqueous, then dried and reused. After five cycles, the conversion of lignin oil was still above 80%, which indicated that the Ru/NC-M catalyst possessed high stability. The reacted Ru/NC-M catalyst was further characterized. The catalyst remains in a layered structure as seen in the SEM image

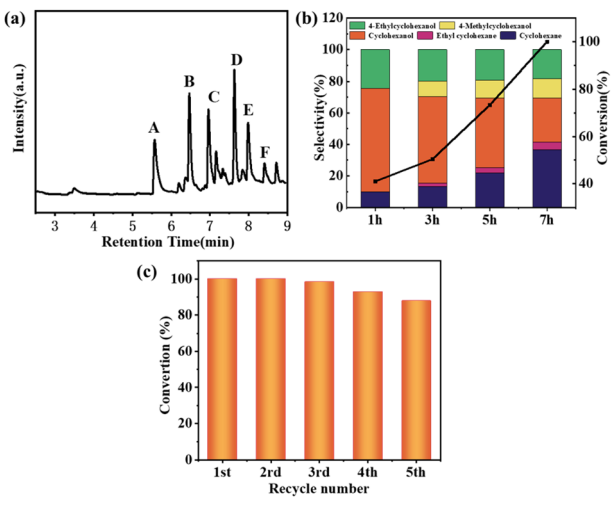

Fig. 5 (a) GC-MS analysis of the main components of lignin oil, (b) hydrodeoxygenation reaction of lignin oil over Ru/NC-M catalyst at different times, (c) cycling experiments of Ru/NC-M catalyst. Reaction conditions: 50 mg lignin oil, 25 mg Ru/NC-M, 30 mL isopropanol, 240 °C, 1 MPa H_2, 7 h, 800 rpm.

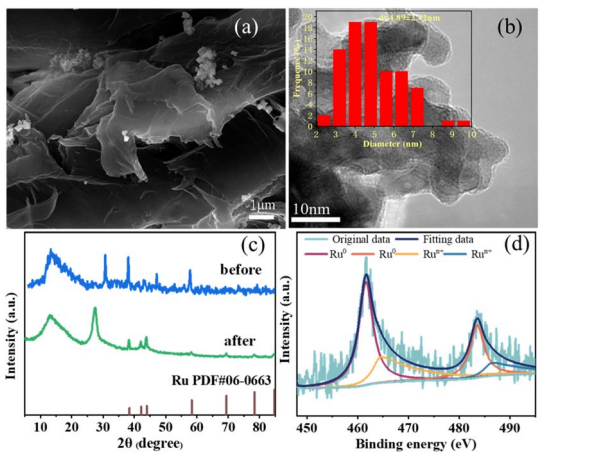

Fig. 6 (a) SEM images, (b) TEM images, (c) XRD patterns and (d) XPS spectra of Ru/NC-M catalyst after reaction. Reaction conditions: 50 mg lignin oil, 25 mg Ru/NC-M, 30 mL isopropanol, 240 °C, 1 MPa H_2, 7 h, 800 rpm.

(Fig. 6a). The metal particles in the catalyst were found to be 4.89 nm according to the TEM characterization, which was slightly increased than before the reaction (Fig. 6b). According to the XRD patterns before and after the reaction of the Ru/NC-M catalyst, it could be seen that the characteristic peaks of Ru metal did not change, which showed that the crystalline shape of the metal did not change, so this Ru/NC-M catalyst had high stability (Fig. 6c). The XPS characterization showed that Ru^0 and Ru^{n+} species were still present in the catalyst with 65.52% and 34.48%, respectively. Therefore, the Ru/NC-M catalyst possesses a strong stability (Fig. 6d).

Analysis of depolymerization products

The depolymerization products on Ru/NC-M (Fig. S4†) were analyzed by GC and GC-MS. The products were cyclohexane, ethyl cyclohexane, cyclohexanol, 4-methyl cyclohexanol, and 4-ethylcyclohexanol, and compared with the composition of lignin oil, it could be seen that the catalyst could not only crack C–O bonds but also hydrogenate aromatic benzene rings.

The chemical structure of the initial lignin oil was characterized by two-dimensional HSQC, and the main side chains and aromatic regions of the 2D HSQC-NMR spectra (δ_C/δ_H200-0/10.0-0) were shown in Fig. 7a, and the signal peaks of guaiacyl (G), syringyl (S), and hydroxyphenyl (H) units were detected in the benzene ring region. At δ_C/δ_H111.7/6.9, δ_C/δ_H115.8/6.7, and δ_C/δ_H119.9/6.8, they correspond to C_2–H_2, C_5–H_5, and C_6–H_6 of the benzene ring of unit G, respectively.

At δ_C/δ_H104.8/6.69, it corresponded to $C_{2,6}$–$H_{2,6}$ of the benzene ring of unit S. At δ_C/δ_H129.5/7.2 corresponds to $C_{2,6}$–$H_{2,6}$ of the benzene ring of unit H (Fig. 7a). In the sidechain region, δ_C/δ_H55.6/3.7 are methoxy signals (Fig. 7b). These signal peaks are absent in the lignin oil depolymerization products produced after the reaction with Ru/NC-M (Fig. 7c). The signal peak of the methyl group corresponds to δ_C/δ_H21.0/2.2, and the signal peak of the ethyl group at δ_C/δ_H30.1/2.8 (Fig. 7d). The Ru/NCM catalyst was found to have a strong C–O bond broken by comparison, especially for hydroxyl and methoxy groups.

Catalytic transformation of lignin model compounds

Guaiacol was a representative lignin model compound, and guaiacol is also contained in lignin oil. In order to further understand the reaction pathway of lignin oil at Ru/NC-M, the catalytic conversion of guaiacol was carried out at 240 °C and 1 Mpa H_2 with Ru/NC-M (Fig. 8).

According to GC-MS analysis, the products were mainly cyclohexanol and 1-methyl-1,2-cyclohexanediol. When the reaction was 1 h, the product was mainly 1-methyl-1,2-cyclohexanediol, only a small amount of cyclohexanol was produced, and the conversion was only 28.77% at this time. As the reaction time increased, the selectivity for 1-methyl-1,2-cyclohexanediol gradually decreased, while the selectivity for cyclohexanol gradually increased. After 4 h of reaction, the conversion of guaiacol was 100%. Based on the above results, the reaction pathway of guaiacol over the Ru/NC-M catalyst was proposed (Fig. 9). The first step was the alkylation and hydrogenation on the benzene ring to convert guaiacol to 1-methyl-1,2-cyclohexadiol. The second step was to hydrolyze 1-methyl-1,2-cyclohexanediol to produce cyclohexanol. The benzene ring of guaiacol was adsorbed on the surface of Ru NPs, and the Brønsted acidic site on the catalyst could transfer the broken O–CH_3 to the benzene ring, which was hydrogenated to produce 1-methyl-1,2-cyclohexanediol, and then hydrolyzed 1-methyl-1,2-cyclohexanediol to produce cyclohexanol. It had been reported that the acidity of the support had a significant effect on the alkyl transfer reaction,[38] which could be observed on catalysts with acidic supports, while the Ru/NC-M catalyst contains acidic sites. This is one of the best results for the hydrodeoxygenation of guaiacol using the same catalyst with only a trace amount of noble metal elements (Table S5†).

Based on the experimental results and literature reports,[39,40] a possible reaction pathway for lignin oil on Ru/NC-M catalyst was proposed, which first performed transalkylation and

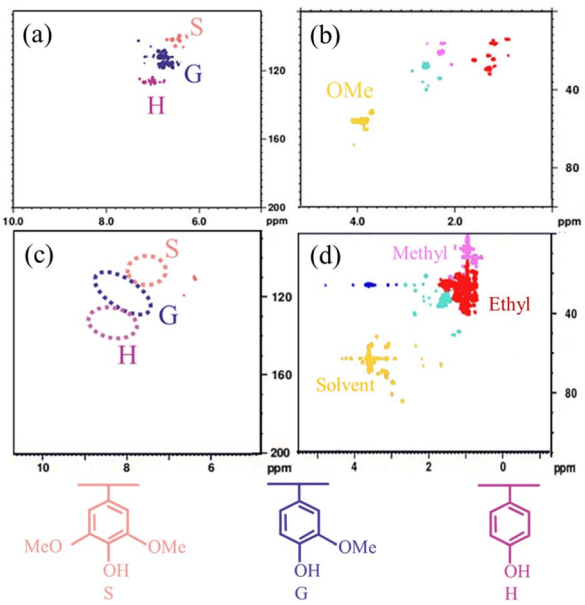

Fig. 7 (a, b) HSQC NMR spectra of Lignin oil. (c, d) HSQC NMR spectra of depolymerized products after hydrogenolysis lignin oil over Ru/NC-M.

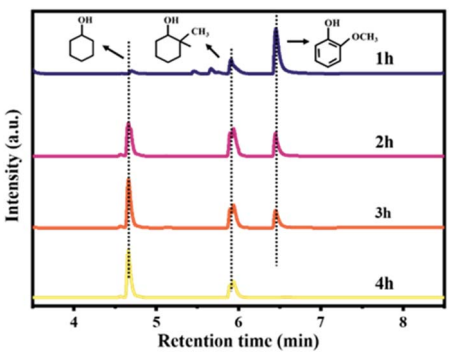

Fig. 8 The effect of different reaction times on the catalytic products. Reaction conditions: 100 mg guaiacol, 50 mg Ru/NC-M, 30 mL isopropanol, 240 °C, 1 MPa H_2, 800 rpm.

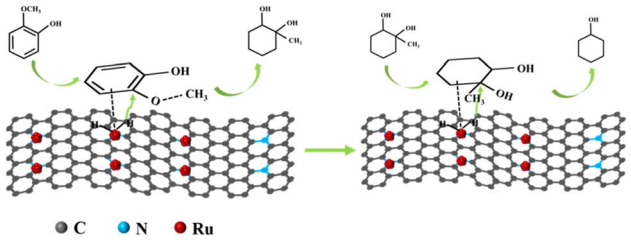

Fig. 9 Proposed pathways of guaiacol over Ru/NC-M catalysts in this work.

hydrogenation reactions on the benzene ring, and then cleaved the C–O bond to finally produce cycloalkane type products. The activation of H_2 was vital in the hydrodeoxygenation reaction.

The presence of pyridine nitrogen could regulate the electron density of Ru NPs, which in turn increases Ru^0 through electron transfer, while the results in Table 1 proved that the active site was the metal Ru, and H_2 was easily activated at the active site to be used for breaking the C–O bonds. In addition, the presence of acidic sites in the catalyst could facilitate the removal of –OH groups and O–CH_3 groups to obtain cyclohexane products.

Conclusion

In summary, the lamellar catalysts by direct pyrolysis of a mixture of metal and nitrogen–carbon precursors were prepared. By altering the nitrogen–carbon precursors, the specific surface area, nitrogen doping type, and the pyridine N content could be adjusted. Nitrogen-doped carbon catalysts immobilized with Ru NPs with high dispersion and small size were synthesized using melamine as the nitrogen–carbon precursor when pyridine nitrogen dominated. There was a significant electronic interaction between N and Ru NPs. The presence of pyridine N not only stabilized and dispersed the Ru NPs as a metal ligand site, but also increased the amount of Ru^0. Enhanced interaction between metal and carrier. Therefore, the catalytic performance of Ru/NC-M catalyst synthesized with melamine as a nitrogen–carbon precursor was stronger than that of catalysts synthesized with urea as a nitrogen–carbon precursor (Ru/NC-U) and dicyandiamide as a nitrogen–carbon precursor (Ru/NC-D). The high-performance Ru/NC-M catalyst could completely degrade lignin oil at 240 °C and 1 MPa H_2, with a selectivity of 36.58% for cyclohexane, and possessed a strong ability to break C–O bonds. The Ru/N-doped carbon catalysts developed in this study were simple to synthesis and provided a promising catalyst for the degradation of lignin oil.

Author contributions

Ma Yulong: conceptualization, resources, writing – review & editing, supervision, project administration, funding acquisition. Zhong Yudan: methodology, software, validation, investigation, writing – original draft. Sun Yonggang: conceptualization, writing – review & editing, methodology, data curation. Wang Liqiong: formal analysis, methodology. Li Yuanyuan: methodology, project administration. Lin Feng: formal analysis. Zhu Yingbo: software, validation.

Conflicts of interest

The authors declare that they have no known competing financial interests or personal relationships that could have appeared to influence the work reported in this paper.

Acknowledgements

The authors thank the Key R&D Projects in Ningxia (Talent Introduction Special Project) (2022BSB03057), the Natural Science Foundation of Ningxia (2023AAC05007) and the National Natural Science Foundation of China (21868026, 22269017) for financial support.

Notes and references

1 C. Chio, M. Sain and W. Qin, *Renewable Sustainable Energy Rev.*, 2019, **107**, 232–249.
2 J. Dillies, C. Vivien and M. Chevalier, *Biotechnol. Appl. Biochem.*, 2020, **67**, 774–782.
3 E. Melro, A. Filipe and D. Sousa, *New J. Chem.*, 2021, **45**, 6986–7013.
4 Z. Chen and C. Wan, *Renewable Sustainable Energy Rev.*, 2017, **73**, 610–621.
5 C. Chen, D. Wu and P. Liu, *React. Chem. Eng.*, 2021, **6**, 559–571.
6 X. Dou, W. Li and C. Zhu, *RSC Adv.*, 2020, **10**, 43599–43606.
7 C. Li, J. Hayashi and Y. Sun, *J. Anal. Appl. Pyrolysis*, 2021, **155**, 105031.
8 Z. Yang, J. Feng and H. Cheng, *Bioresour. Technol.*, 2021, **321**, 124440.
9 G. Guo, W. Li and T. Ahmed, *RSC Adv.*, 2021, **11**, 37932–37941.
10 A. Manas, N. Chaussard and F. Bertaud, *Ind. Eng. Chem. Res.*, 2022, **61**, 7430–7437.
11 K. Zhang, H. Li and L. P. Xiao, *Bioresour. Technol.*, 2019, **285**, 121335.
12 F. Lin, Y. Ma and Y. Sun, *Renewable Energy*, 2021, **170**, 1070–1080.
13 F. Lin, Y. Ma and Y. Sun, *Renewable Energy*, 2022, **189**, 1278–1291.
14 C. Liu, C. Zhou and Y. Wang, *Proc. Combust. Inst.*, 2021, **38**, 4345–4353.
15 L. Pastor-Pérez, W. Jin and J. J. Villora-Picó, *J. Energy Chem.*, 2021, **58**, 377–385.
16 M. Buffi, A. Cappelletti and A. M. Rizzo, *Biomass Bioenergy*, 2018, **115**, 174–185.
17 R. Kumar and V. Strezov, *Renewable Sustainable Energy Rev.*, 2021, **135**, 110152.
18 S. De, B. Saha and R. Luque, *Bioresour. Technol.*, 2015, **178**, 108–118.
19 M. Auersvald, B. Shumeiko and D. Vrtiška, *Fuel*, 2019, **238**, 98–110.
20 K. L. Lu, F. Yin and X. Y. Wei, *Mol. Catal.*, 2023, **534**, 112806.

21 H. Yang, L. Wang and S. Xu, *Chem. Eng. J.*, 2022, **431**, 133863.
22 T. Li, H. Lin and X. Ouyang, *ACS Catal.*, 2019, **9**, 5828–5836.
23 J. H. Advani, H. K. Noor-ul and H. C. Bajaj, *Appl. Surf. Sci.*, 2019, **487**, 1307–1315.
24 Z. Dou, Z. Zhang and H. Zhou, *Angew. Chem., Int. Ed.*, 2021, **60**, 16399–16403.
25 N. T. T. Tran, Y. Uemura and A. Ramli, *Mol. Catal.*, 2022, **523**, 111435.
26 G. Wen, Q. Gu and Y. Liu, *Angew. Chem., Int. Ed.*, 2018, **57**, 16898–16902.
27 Y. Ishii, K. Ishigame and Y. Kido, *RSC Adv.*, 2019, **9**, 42043–42049.
28 H. Chen, K. Shen and Q. Mao, *ACS Catal.*, 2018, **8**, 1417–1426.
29 T. Li, H. Lin and X. Ouyang, *Fuel*, 2020, **278**, 118324.
30 R. Zhao, Z. Liang and S. Gao, *Angew. Chem.*, 2019, **131**, 1997–2001.
31 Z. Zhang, S. Yao and X. Hu, *Adv. Sci.*, 2021, **8**, 2001493.
32 F. Li, L. J. France and Z. Cai, *Appl. Catal., B*, 2017, **214**, 67–77.
33 Y. Qi, X. Xiao and Y. Mei, *Adv. Funct. Mater.*, 2022, **32**, 2111615.
34 G. Yao, G. Wu and W. Dai, *Fuel*, 2015, **150**, 175–183.
35 P. Liu, C. Chen and M. Zhou, *Sustainable Energy Fuels*, 2021, **5**, 1809–1820.
36 X. Wang, C. Li and X. Guo, *Front. Chem.*, 2022, **10**, 961814.
37 K. L. Lu, F. Yin and X. Y. Wei, *Mol. Catal.*, 2023, **534**, 112806.
38 X. Fan, Y. Wu and R. Tu, *Renewable Energy*, 2020, **157**, 1035–1045.
39 C. Huang, Y. Su and J. Shi, *New J. Chem.*, 2019, **43**, 3520–3528.
40 M. Zhou, J. Ye and P. Liu, *ACS Sustainable Chem. Eng.*, 2017, **5**, 8824–8835.